Colloids and Surfaces A: Physicochemical and Engineering Aspects 660 (2023) 130849

Contents lists available at ScienceDirect

Colloids and Surfaces A: Physicochemical and Engineering Aspects

journal homepage: www.elsevier.com/locate/colsurfa

Identification of an optimized ratio of amyloid and non-amyloid fractions in engineered fibril solutions from whey protein isolate for improved foaming

Jacqueline Lux [a], Helena Kieserling [b,d], Jörg Koop [c], Stephan Drusch [d], Karin Schwarz [a], Julia K. Keppler [a,e], Anja Steffen-Heins [a,*]

[a] Institute of Human Nutrition and Food Science, Divison of Food Technology, Kiel University, Germany
[b] Institute of Food Technology and Food Chemistry, Department of Food Chemistry and Analysis, Technische Universität Berlin, Germany
[c] Department of Biochemical and Chemical Engineering, Laboratory of Plant and Process Design, TU Dortmund University, Germany
[d] Insitute of Food Technology and Food Chemistry, Department of Food Biotechnology and Process Engineering, Technische Universität Berlin, Germany
[e] Laboratory of Food Process Engineering, Wageningen University, Wageningen, the Netherlands

HIGHLIGHTS

- Non-amyloid fraction dominates adsorption behavior in fibril systems.
- Small amounts of amyloid aggregates are necessary to stabilize foams.
- Non-amyloid material is embedded into fibrillar network at the air-water interface.
- Orientation of semi-flexible protein fractions at the interface is energy consuming.
- Interplay of both fractions reduces protein concentration for foam stabilization.

GRAPHICAL ABSTRACT

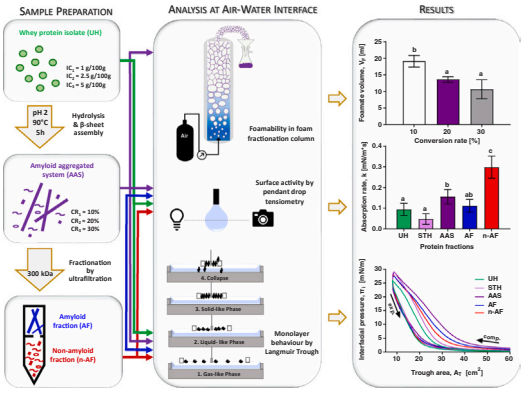

ARTICLE INFO

Keywords:
Amyloid aggregates
Fibrils
Non-amyloid material
Pendant drop analysis
Langmuir trough
Air-water interface

ABSTRACT

Engineered fibril solutions from whey protein beta-lactoglobulin are known for their excellent foaming capacity. These amyloid aggregates solutions (AAS) usually contain a polydisperse mixture of different protein structures. An optimized ratio of amyloid (AF, fibrils) and non-amyloid fractions (n-AF) in AAS may improve foaming, particularly by interactions at the air-water interface. Foamability, surface activity, and monolayer phase behavior at the air-water interface of isolated AF and n-AF as well as AAS with different AF/n-AF-ratios were investigated using drop tensiometry, Langmuir trough and foam analysis. N-AF exhibited faster migration, twice as fast adsorption and thus faster spreading at the air-water interface than the fibrils (AF). N-AF required less energy to assemble in a liquid-expanded phase in a monolayer, i.e., they were more compressible in the monolayer than AF. This resulted in rapid stabilization of lamellae in foam. High surface hydrophobicity of AF

Abbreviations: AAS, amyloid aggregate system; AF, amyloid fraction; β-lg, beta-lactoglobulin; G, gas-like distribution; LC, liquid condensed phase; LE, liquid expanded phase; n-AF, non-amyloid fraction; PAI, pressure-area isotherms; STH, short time heated WPI; UH, unheated WPI at pH 2; WPI, whey protein isolate.

* Correspondence to: Institute of Human Nutrition and Food Science, Division of Food Technology, Heinrich-Hecht-Platz 10, D-24118 Kiel, Germany.
E-mail address: aheins@foodtech.uni-kiel.de (A. Steffen-Heins).

https://doi.org/10.1016/j.colsurfa.2022.130849
Received 4 November 2022; Received in revised form 18 December 2022; Accepted 21 December 2022
Available online 26 December 2022

results in faster adsorption and formation of capillary forces between adsorbed fibrils, improving the attraction for additional fibrils. Orientation of semi-flexible and larger fibrils in AF consumes high energy. In combination with n-AF, the energy needed for orientation and assembly of fibrils is equivalent, however, the yield of AF in AAS was only 20 %, indicating the interplay of amyloid and non-amyloid proteins at the air-water interface. N-AF can be incorporated into a fibrillar film, which increase the network's density and stiffness and the interfacial film stability. Consequently, in AAS fibrils and non-amyloid material acted synergistically at the air-water interface, whereby only small amounts of amyloid aggregates are required to stabilize foams.

1. Introduction

Bovine whey protein isolate (WPI) consists mainly of beta-lactoglobulin (β-lg > 58 %) and shows high surface activity, i.e., gelling, emulsifying, foaming and film formation capacity. These properties can be improved by tailored structuring of proteins, e.g., amyloid aggregation, resulting in engineered amyloid fibrils with condition-dependent morphology [1], as has been comprehensively reviewed elsewhere [1–3]. Typical studied conditions to prepare amyloid fibrils from β-lg or WPI are thermal treatment for at least five hours at ~90 °C, pH 2 and low ionic strength [2,4]. This leads to hydrolyzed β-sheet peptides, which self-assemble into semi-flexible fibers of several micrometers in length and several nanometers in width. However, not all of the formed peptides are converted into fibrils, so that under the described conditions only 25–30 % β-lg aggregate while the rest consists of non-amyloid aggregates, peptides and monomers [1,5]. In order to accurately analyze the effect of fibrillation on technological functions, most studies dealing with isolated fibrils purified them by dialysis or ultracentrifugation [6–9]. Isolated β-lg amyloid fibrils adsorb at oil-water and at air-water interfaces, leading to nematic domains and highly elastic films [6,10]. The fibrillar structure of β-lg reduces the interfacial tension more rapidly than the native protein [6]. At high concentrations of isolated amyloid fibrils at the air-water interface, a decrease in interfacial elasticity was observed, which is attributed to a multilayer adsorption and fibril fracture in the topmost layer [10]. However, Peng and colleagues [8] reported that foams of isolated fibrillated β-lg at pH 2 were physically less stable to coalescence, coarsening, and prevention of air diffusion owing to a less densely packed layer around the bubbles. Hu et al. [9] pointed out that the most important parameter for foam stability seems to be high interfacial elasticity which most likely occurs at pH 4, close to the isoelectric point, for various β-lg aggregates.

Interfacial properties of engineered amyloid fibrils have attracted much attention in the food industry because of their high foaming capacity at low protein concentrations [3,11,12]. Because of the low physical stability of foams with isolated β-lg fibrils [8], it is of great interest to understand the interaction between protein fibrils and the remaining non-fibrillated material at the air-water interface. Recently, Yue and colleagues [2] pointed out in their review that it is the non-amyloid structures that have a significant contribution to the techno-functional properties of fibrillated protein systems, as also shown in studies with rice bran protein [13,14] and WPI [12]. At a pH value of 7, Rullier and colleagues [15] suggested the formation of a synergistic network between β-lg aggregates and the remaining non-aggregated material. They also demonstrated that the particle size of the aggregates as well as the ratio between aggregates and the non-aggregated proteins are crucial for the formation of a viscoelastic gel-like network in the interfacial film [16]. For a soy glycine fibril system containing amyloid aggregates as well as non-amyloid proteins and peptides, there is first evidence that the interfacial tension and foaming behavior is comparable to that of isolated peptides irrespective of the pH value. However, isolated soy glycine fibrils reduce interfacial tension more slowly and weakly than the whole fibril system, resulting in lower foam stability [17]. A higher foam stability because of a higher viscosity and a gel-like network at the air-water interface in pH-structured compared to untreated protein solutions were already observed for fibrillated WPI solution at pH 2 [18], 4 and 6 [19] or aggregated WPI solutions at pH 7 [20].

Overall, there is evidence in the literature that the mixture of fibrils and non-amyloid material can improve foam stability regardless of the origin of the protein [3]. However, experimental data on the interaction of fibrils and non-amyloid protein materials at the air-water interface are limited [2], particularly for evaluating the function of the non-amyloid structures. With regard to the foaming properties of fibrillated WPI solutions, we aim at defining an optimized ratio of amyloid and non-amyloid structures for foaming. For this reason, we evaluated the behavior of the complete amyloid system (AAS) at the air-water interface in comparison to its isolated fractions, i.e. amyloid aggregated fibrils (AF) and the remaining non-amyloid material (n-AF).

We hypothesize that the n-AF, containing aggregate fractions and peptides, plays an important role by interacting with fibrils at pH 2 and may improve the stability of this system at the air-water interface. Because of the faster adsorption at the air-water interface, small proteins [16], are able to occupy the interface first and facilitate the subsequent attachment of fibrils which will form a network.

We further propose that the use of fibrillated WPI without removal of non-amyloid material improves foamability and foam stability, where an optimized ratio of amyloid and non-amyloid fractions can be achieved by varying the initial WPI concentrations. Acid hydrolysis at pH 2.0 is rate-limiting. With a higher initial WPI concentration, more peptides are formed in general, but also significantly more longer peptides in which N- and C-terminal segments are still connected [21]. These peptide segments favor fibril formation and consequently increase the conversion rate.

Aggregating WPI at different protein concentrations at pH 2 and 90 °C for 5 h, we obtained AAS with varying conversion rates. Fractions (AF, n-AF) were separated by ultrafiltration (MWCO = 300 kDa). Unheated (UH) and a short time heated WPI sample (STH) was used as controls at pH 2. STH corresponds to a partly denatured but non-hydrolyzed sample. AAS with different conversion rates into fibrils were compared with the isolated fractions and investigated in terms of adsorption kinetics on the air-water interphase using pendant drop tensiometry and film formation using Langmuir trough. Finally, the foamability and foam stability of the amyloid fibrils were evaluated by performing foam fractionation experiments in a foam fractionation column.

2. Materials and methods

2.1. Materials

The whey protein isolate BiPro (total protein content ≥ 95 % dry matter basis, HPLC analysis quantified ~77 % β-lg, ~21 % α-lactalbumin (α-la), ~2 % bovine serum albumin) was purchased from Davisco Foods International (Eden Prairie, Minnesota, USA). Ultrapure water (18.25 MΩ cm) was obtained from a Milli-Q system and used for sample preparations and experiments. Hydrochloric acid was purchased from Carl Roth (Karlsruhe, Germany) and used without further purification.

2.2. Sample preparation

2.2.1. Preparation of WPI amyloid aggregates

Preparation of fibrillated WPI solution was carried out according to Serfert et al. [22]. A WPI solution at a concentration of 2.5 g/100 g was adjusted to pH 2 with 6 mol/l HCl. For fibril formation, the WPI solution was heated at 90 °C for 5 h under stirring (350 rpm, 2mag MIXdrive 6HT, 2mag AG, Munich, Germany).

Two different WPI controls were prepared. The unheated control (UH) consisted of native WPI solution adjusted to pH 2. The short time heated control (STH) was additionally heated for 30 min at 90 °C. Sampling was performed at three different times. The five hours heating resulted in the amyloid aggregate system (AAS) consisting of the amyloid fraction (AF) and the non-amyloid fraction (n-AF). After five hours the fibril formation was almost complete and all proteins were unfolded [5]. Solutions were cooled on ice and stored at 4 °C until further use. Additional experiments were carried out by varying the protein concentration from 1 to 5 g/100 g. For the analysis, all dilutions were carried out with MilliQ water, adjusted to pH 2 with HCl.

2.2.2. Separation of individual fractions by ultrafiltration methods

To separate the AF from the n-AF as far as possible, the AAS was diluted 5-fold and filtered with ultrafiltration centrifugal concentrators (Vivaspin 20, 300 kDa, PES, Sartorius, Göttingen, Germany). The concentrators were washed with pH-adjusted water. 10 ml of the diluted sample was filled in the washed concentrators, weighted and centrifuged for 15 min at 1000 x g at room temperature. After each centrifugation step the retentate was refilled with pH 2-water up to the initial weight and the protein adhering to the membrane was scratched with a plastic spatula, the procedure was repeated three times. The filtrates from all filter steps were collected as n-AF. The retentate of the last centrifugation step was filled up to the initial volume with pH 2 water and hereafter AF.

2.2.3. Measurement of conversion rate

The conversion rate from β-lg into amyloid aggregates prepared with initial protein concentrations of 1 g/100 ml, 2.5 g/100 ml, and 5 g/100 ml was determined according to Serfert et al. [22]. The AAS were diluted to 0.1 g/100 ml protein concentration and filtered with ultrafiltration centrifugal concentrators (Vivaspin 2, 300 kDa; Sartorius GmbH, Göttingen, Germany). The samples were washed three times with pH 2-water. The conversion rate was defined as the protein, which remains in the retentate after ultrafiltration. The protein concentration was measured at 278 nm using a UV-Vis spectrometer (Helios Gamma, UV-Vis, Thermo Spectronic, Cambridge, UK) in a quartz cell and calculated by a calibration curve for WPI at pH 2. For further measurements, all samples were diluted to the same protein concentration.

2.3. Analytical methods

2.3.1. Langmuir trough measurements

The pressure-area isotherms (PAI) and the adsorption kinetics at the planar interface were recorded with a Langmuir trough (Modell: 611D, NIMA Technology, UK). 50 ml water adjusted to pH 2 was used as sub phase. For the PAI, 50 μL of a 0.01 g/100 ml protein solution was applied dropwise on the surface and equilibrated for 15 min. During compression of trough area to 8 cm^2 and expanded to 94 cm^2 with a speed of 0.358 cm^2 s^{-1}, the surface pressure was measured. All measurements were carried out in triplicate. The phase transitions were analyzed graphically by spotting drastic change in slope from the first derivative of the separate compression and expansion isotherms. The hysteresis loop areas between the compression and expansion isotherm were calculated from the difference of the respective area under the curves (units: 10^{-3} N/m * 10^{-4} m^2 = 10^{-7}Nm = 0.1 μNm = 0.1μJ).

2.3.2. Pendant drop tensiometry

The interfacial tension of AF, n-AF and AAS (1 g/100 ml, 2.5 g/100 ml, 5 g/100 ml) against air was measured with an automated drop tensiometer (OCA20, Dataphysics GmbH, Germany), equipped with a high-speed camera (200 frames/second). Therefore, a two-fluid needle system was used as described by Tamm and colleagues [23] with slight modifications. Through a large needle (d = 1.65 mm), 14 μL of water was dosed manually, whereas 1 μL of 0.15 g/100 ml fibrils/non-fibril solution was dosed by an automatic injection system through a small needle (d = 0.51 mm) into the initial water droplet. The total protein concentration was 0.01 g/100 ml. In accordance with Schestkowa et al. [24], lag time through the bulk phase, adsorption, and reduction of the interfacial tension were analyzed by nonlinear regression using GraphPad Prism (version 6.07, GraphPad Software, San Diego, CA, USA).

2.3.3. Foaming properties

The foaming experiments were performed in a glass foam fractionation column (lower part: 130 mm length, 35 mm inner diameter; upper part: 420 mm length, 20 mm inner diameter), for schematic view see [25]. The AAS with an initial protein concentration of 1, 2.5 and 5 g/100 ml were used and diluted to a final concentration of 0.01 g/100 ml. 90 g of the 0.01 g/100 ml AAS solution was used as feed solution. The solution was sparged with gas by a porous glass frit P3 of a pore size 16–40 μm (ROBU, Hattert, Germany) located in the bottom of the column. The airflow was set to 7 l/h. The foaming was conducted until the continuous foam flow was interrupted by large holes formed due to lamella rupture and coalescence. The foamate and the retentate were collected, weighted and the protein concentration was measured at 278 nm wavelength using a UV-Vis spectrometer (Spectro 50, Analytik Jena AG, Jena, Germany) in micro UV cuvettes (BRAND, Wertheim, Germany). The foamabiliy was indicated by the volume of the foamate (V_F) and V_F/time as surface activity indicator [26]. High foam stability was indicated by a low protein concentration in the retentate. Because of this concentration is defined by the point at which the foam collapses, thus ending the experiment, a low protein concentration implies a large foam stabilization capability of the protein.

2.4. Statistical analysis

If not stated otherwise, all results were presented as mean and standard deviation of the replicated sample preparations and analyses. For the replicates, normal distribution could be assumed according to the Shapiro-Wilk test ($p > 0.05$). The equality of variances was confirmed using Brown-Forsythe test. Significant differences were identified by one-way ANOVA with Tukey's multiple comparison test at least at a significance level of $p = 0.05$. All statistics and figures were created using GraphPad Prism (version 9.1, GraphPad Software, San Diego, CA, USA).

3. Results & discussion

3.1. Fractions of amyloid and non-amyloid peptides after thermal aggregation as a function of initial WPI concentration

Increasing initial WPI concentrations for the aggregation process at pH 2 and 90 °C resulted in increasing conversion rates (Fig. 1). An initial protein concentration of 1 g/100 g solvent led to the formation of 10.6 ± 4 %, 2.5 g/100 g to 18.2 ± 0.03 % and 5 g/100 g to 27.5 ± 1.1 % amyloid fibrils, while the respective remaining fraction consisted of non-amyloid aggregates and peptides. For simplicity, the following results investigating the AAS the yield of fibrils in terms of initial WPI concentration used are referred to as conversion rates of 10 %, 20 %, and 30 %.

The results evidenced that the ratio between fibrils and non-amyloid protein material can be adjusted by the initial protein concentration. This can be attributed to acid hydrolysis of peptide bonds at pH 2 as a

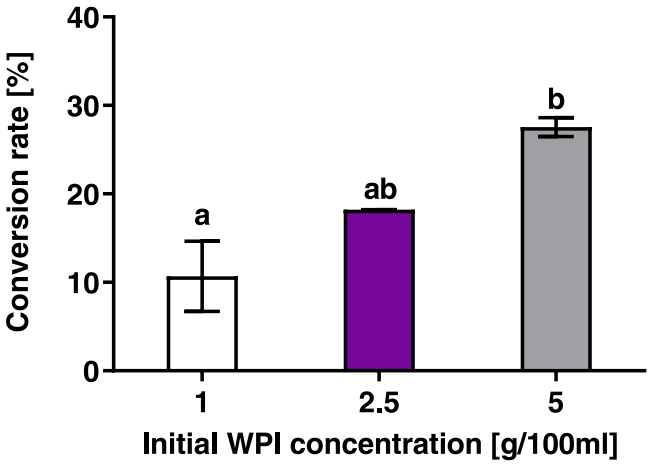

Fig. 1. Conversion rates of WPI into amyloid aggregates as a function of the initial protein concentration, given as the protein concentration in the retentate after ultrafiltration relative to the total protein concentration (also amyloid fraction, AF). Prior to UF, these total amyloid aggregated systems (AAS) were diluted to the same protein concentration of 0.01 g/100 ml. Different letters indicate significant differences ($p < 0.05$, Tukey).

rate-limiting step in the same time scale as fibril formation [21]. Ye and colleagues stated that with increasing protein concentration, on average more longer peptide fragments are formed, with the N-terminal and C-terminal peptides still connected. These may be either proteins that are still intact or, more likely, peptides that are still connected via C^{66}-C^{160} disulfide bonds. Stronger embedding of the C-terminal peptides favors fibril formation and, consequently, the shift in the ratio between AF than n-AF. This was in line with the findings of Bolder and colleagues [27]. However, the thermal treatment lasted for 10 h at 80 °C and 5 g/100 g WPI revealed a higher conversion rate (~45 %). Also Veermann and colleagues [28], reported higher conversion rates ranging from 45 % to 60 % for 1–4 g purified ß-lg/100 ml, respectively. In both studies the authors quantified the amyloid fraction by removing all aggregates, which were insoluble at pH 4.8. However, in this way the particle size was not taken into account and non-amyloid aggregates may have erroneously increased the conversion rate. Using the same conditions for amyloid aggregation and conversion rate analysis as described in our experimental set-up, for a 2.5 g/100 ml pure β-lg solution conversion rates of ~30 % [29] and ~25 % [5], were found, respectively. As the β-lg content of WPI used in the present study was 77 %, a conversion rate of ~18 % at a protein concentration of 2.5 g/100 ml is roughly consistent with Heyn et al. [5] and supported the observation that only β-lg from the WPI contributes to fibril formation [30].

Using a molecular weight cut off of 300 kD for ultrafiltration results in AF consisting primarily of fibrils and large aggregates, while the n-AF contains mainly non-amyloid aggregates, peptides and remaining unfolded protein < 300 kDa [5]. In a previous study we demonstrated by electron spin resonance spectroscopy for the same procedure that some non-amyloid aggregates and peptides were present in both fractions because they possibly are enclosed in the filter cake and thus remain in the AF [31]. In addition, the n-AF may also contain fragments of fibrils destroyed during the filtration step [4]. However, after ultrafiltration at 300 kDa we can clearly rule out the presence of amyloid material in the obtained n-AF [31,32].

3.2. Adsorption kinetics at the air-water interface of the entire amyloid aggregated systems as a function of conversion rates and its isolated fractions

The interfacial activity of AAS at varying ratios of amyloid and non-amyloid fractions was evaluated by pendant drop analysis. Migration of total protein material towards the air/water interface (Fig. 2A), its adsorption rate (Fig. 2B) and the resulting interfacial pressure (Fig. 2C) were investigated. The migration was reported as the lag time. It represents the time between sample injection into the droplet and the time point, at which the interfacial tension begins to decrease. Regardless of the conversion rate, the lag times were equal for all samples with an averaged migration time of 24.1 ± 5.9 s (Fig. 2A). The individual adsorption rate at the air/water interface, deduced from the slope of decreasing interfacial tension, ranged from $k_{20\,\%} = 0.15 \pm 0.03$ mN/m·s to $k_{30\,\%} = 0.21 \pm 0.05$ mN/m·s and did not differ significantly (Fig. 2B). The difference between pure water (mean $\sigma_w = 72.3 \pm 0.3$ mN/m) and after adsorption of AAS at the air-water interface (mean $\sigma_p = 58.8 \pm 0.5$ mN/m) is also referred to as the interfacial pressure ($\Pi_i = \sigma_w - \sigma_p$). Regardless of the conversion rate, all samples exhibited a mean interfacial pressure of $\Pi_i = 13.1 \pm 0.9$ mN/m when the air-water interface was fully occupied by protein material (Fig. 2C). Thus, the different ratios of amyloid and non-amyloid proteins in AAS revealed equal surface activity, however, replicates showed high variation.

The interfacial activity of the isolated fractions AF and n-AF from AAS with a conversion rate of 20 % (Fig. 3) was compared. Two structurally different samples served as non-aggregated controls. The unheated control (UH) consisted of native WPI solution adjusted to pH 2 to account for pH-dependent changes in native β-lg, such as its presence as monomers and its highest net charge (+ 20 mV). The short time heated control (STH) was additionally heated for 30 min at 90 °C, resulting in a mostly unfolded but non-hydrolyzed protein. It is noteworthy that the interfacial tension curves differ in their slopes and also in scattering of replicates (*supp. material* Fig. S1). While values for STH and AAS exhibited high variation, values for UH as well as for isolated AF and n-AF were closer to each other. This indicates heterogeneity of the protein material after thermal treatment, whereas a more homogeneous peptide and aggregate size distribution can be expected after fractionation. The heterogenous protein material migrated and adsorbed at different rates to the interface dependent on molecular weight, surface hydrophobicity, charge anisotropy and molecular flexibility of the individual particles [27,28,33,34].

Comparison of the lag time showed that both control samples UH ($t = 47.8 \pm 14.3$ s) and STH ($t = 44.7 \pm 12.2$ s) took twice as long as all amyloid solutions to migrate through the bulk phase to the air-water interface (Fig. 3A, averaged $t = 21.7 \pm 6.2$ s). This confirmed the expected high surface activity of the fibrillated WPI compared to unheated WPI. However, it was unexpected that the lag time did not differ among AAS, AF and n-AF. The lag time depends mainly on the migration velocity in the bulk and therefore corresponds with the size of the proteins. Because AAS and AF contain large aggregates > 300 kDa, a slower migration to the interface was expected than for the hydrolyzed n-AF fraction. For denatured and aggregated β-lg, a slower migration to the interface and a slower adsorption rate than for native β-lg has already been described [15,34]. However, it should be taken into account that in the present set-up convection of proteins and peptides occurred during sample dosing into the droplet. This may superimpose differences in migration and lead to equal lag times [24,35].

The adsorption of the different protein structures was significantly faster for aggregated samples than for STH and UH (Fig. 3B). N-AF ($k = 0.30 \pm 0.05$ mN/m·s) was three times faster than STH and UH (average $k = 0.07 \pm 0.03$ mN/m·s) and twice as fast as AAS ($k = 0.14 \pm 0.04$ mN/m·s). Isolated fibrils (AF, $k = 0.11 \pm 0.03$ mN/m·s) adsorbed significantly slower than the isolated n-AF. The slow adsorption of the UH and STH may be explained by the low molecular flexibility of the globular protein at pH 2. Conformational changes and a rearrangement of the tertiary structure are restricted [33,36], while simultaneously at pH 2 repulsion effects of the highly charged protein occur. Such repulsion effects are likely to be less pronounced with an anisotropic charge distribution as in long fibrils or heterogenous peptides. The lower surface hydrophobicity of n-AF [4,5] could be balanced out by its higher molecular flexibility. For freeze dried n-AF, a higher zeta potential was

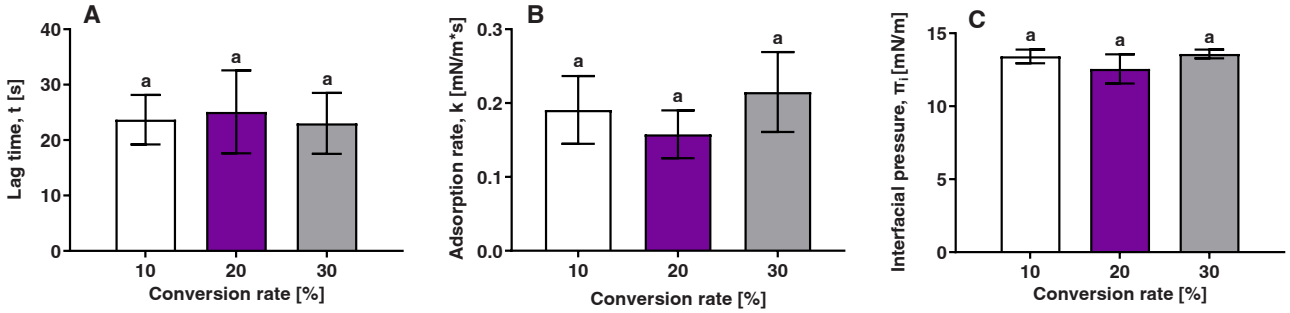

Fig. 2. Pendant drop measurements of whey protein isolate solution at pH 2, heated for 5 h at 90 °C (AAS), with different conversion rates of approx. 10 % (white), 20 % (purple), or 30 %(grey). (A) Migration expressed as lag time (t), (B) adsorption rate (k) at the air-water- interface and (C) interfacial pressure (Π_i) in the state of a fully occupied air-water interface by proteins. Prior to measurements, all samples were adjusted to a final protein concentration of 0.01 g/100 ml. Different letters indicate statistically significant differences (n = 3, $p < 0.05$, Tukey).

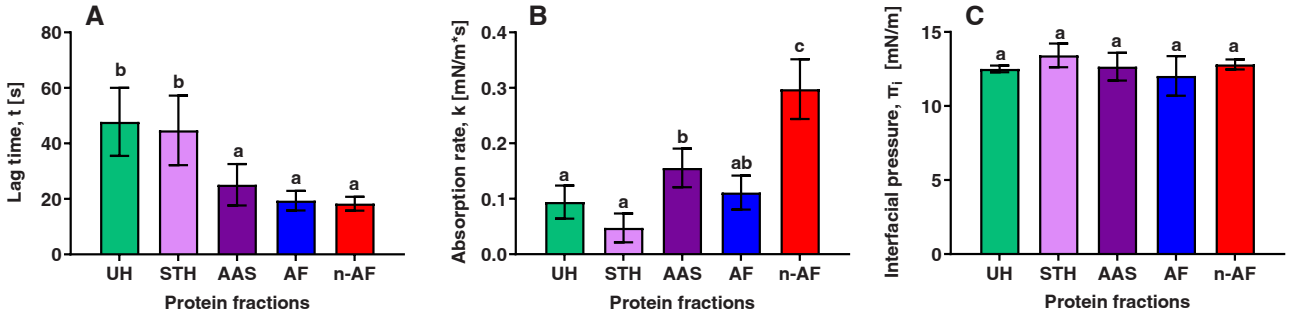

Fig. 3. Pendant drop measurements of whey protein isolate solution at pH 2, heated for 5 h at 90 °C (AAS) and for individual protein fractions and controls of unheated (UH, green) and short time (30 min) heated (STH, light purple) WPI. The amyloid fraction (AF, blue) and the non-amyloid fraction (n-AF, red) were isolated from AAS with a conversion rate of approx. 20 % (purple). (A) Migration (B) adsorption rate at the air-water interface and (C) interfacial pressure (Π_i) in the state of a fully occupied air-water interface by proteins. Prior to measurements, all samples were adjusted to a final protein concentration of 0.01 g/100 ml. Different letters indicate statistically significant differences (n = 3, $p < 0.05$, Tukey).

observed, as well as lower Nile red activity, as a direct measure for surface hydrophobicity, than the AF and AAS [5]. At the same time, the lower molecular flexibility of the large fibrils in AF can be compensated by the high surface hydrophobicity, followed by the formation of capillary forces between adhered fibrils attracting further fibrils. Thus, AAS, n-AF, and AF ultimately exhibited similar surface activity, evidenced by similar decrease in interfacial tension. An average interfacial pressure of $\Pi_i = 12.7 \pm 0.9$ mN/m was found for the fully occupied air-water interface for all samples (Fig. 3C).

3.3. Monolayer phase behavior of protein fractions at the air-water interface as a function of amyloid and non-amyloid components

The behavior of adsorbed protein fractions at the air-water- interface was investigated during its compression and expansion using a Langmuir trough given by the interfacial pressure – area isotherms (Π_i-A_T). The area (A_T) corresponds to the trough area in cm^2, as the commonly used mean molecular area in $Å^2$ varied by hydrolysis and structural changes during the thermal aggregation (Fig. 4A). During 20 min spreading of the proteins, the interfacial pressure reached an equilibrium at a mean interfacial tension of $\sigma_i = 67.8 \pm 2.1$ mN/m. All protein fractions showed strong film formation at the air-water interface with surface pressure greater than $\Pi_i > 25$ mN/m at full compression, which is comparable to the condensed monolayer phases of human and bovine serum albumin [37,38]. Compression of the air-water interface increased the interfacial pressure of the aggregated samples faster than that of the controls and exhibited different phase transition time points of the monolayers as can be derived from the slopes by the first derivatives of Π_i-A_T isotherms (*supp. material* Fig. S2a). Rapid changes in slopes are indicative of the phase transitions of the condensed monolayer [39], which is often represented in literature in compressibility modulus C^{-1}, where the slope is additionally multiplied by the negative mean molecular area [40](*supp. material* Fig. S2b). A gas-like distribution (G) of molecules is assumed during the exponential increase until the molecules collide. At this specific area, in which the compression of the molecules begins ($A_{T\text{-}LE}$), the slope turned linearly indicating the transition from G to a liquid-expanded monolayer (LE), i.e., the restriction of the molecular orientation with respect to each other [38]. This LE transition was reached in the following order: AAS ($A_{T\text{-}LE} = 28.2 \pm 3.3$ cm^2) > AF ≥ n-AF ≥ STH > UH ($A_{T\text{-}LE} = 19.3 \pm 1.3$ cm^2) (Fig. 3B). For comparison, the trough area of these LE transitions were found to correspond very well with those of a fully occupied air-water interface at an interfacial pressure of $\Pi_i = 12.7 \pm 0.9$ mN/m (Fig. 4B and Fig. 3C). Thus, the alignment of the proteins occurred in 2D direction, and the AAS and AF occupied more space at the air-water interface according to their size. The anticipated space requirement of proteins in UH and STH at the air-water interface is much smaller, because native β-lg at pH 2 is predominantly present as monomers and in molten globule state [41], and its tight folding [42] also resulted in a low surface adsorption capacity at low pH values [36]. Contrary to that, the acidic hydrolyzed peptides of the n-AF revealed an open conformation [5] and may probably freely spread on the surface [38], also occupying significantly larger area than native β-lg. These observations on the spatial requirements of the different structures were also consistent with their molecular flexibility. The linear slope of AAS isotherm ($\frac{\delta \Pi_i}{\delta A_T} = -1.0$) and its isolated fibrils in LE state were significantly flatter compared with controls STH ($\frac{\delta \Pi_i}{\delta A_T} = -1.7$) (Fig. 4C). This is most likely an indication of higher resistance of the thermally treated samples towards compression, which could be due to a longer-lasting alignment of the less flexible fibrils at the air-water interface. This means that the most

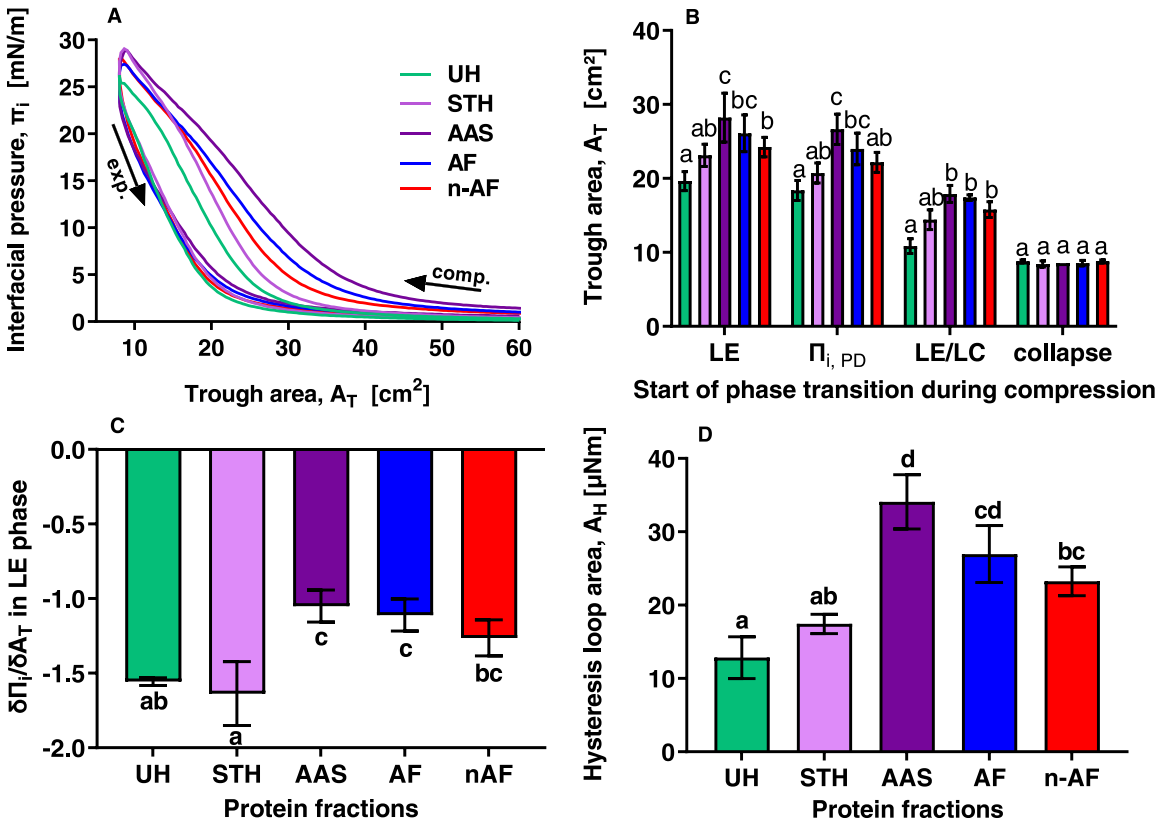

Fig. 4. (A) Pressure-area isotherms (Π_i-A_T) of spread WPI monolayers with different thermal treatment and fractionation: unheated (UH), short time (30 min) heated (STH) and WPI heated for 5 h at 90 °C (AAS) with a protein concentration of 2.5 g/100 ml (conversion rate approx. 20 %). The amyloid fraction (AF) and the non-amyloid fraction (n-AF) were isolated from AAS accordingly. The area of Langmuir trough area was compressed and expanded between 94 cm^2 and 8 cm^2 after 20 min equilibration. (B) Starting points of phase transitions from the gaseous to the liquid-expanded state (LE), and to the state of LE and liquid-condensed (LC) coexistence phase (LE/LC), as well as to the collapse of the condensed monolayer. For comparison the point of interfacial pressure of fully occupied interface analyzed by pendant drop ($\Pi_{i,PD}$= 12.7 mN/m). (C) Slopes of compression isotherms in the LE state. (D) Energy required for protein orientation at the interface, calculated by the area of the hysteresis loop. Different letters indicate statistically significant differences (n = 3, $p < 0.05$, Tukey).

flexible and least structured protein showed the steepest slope, as it was indeed the case for STH, followed by UH, n-AF, and AF. The significantly earlier LE transition (Fig. 4B) and lower flexibility (Fig. 4C) of the AAS compared with isolated fractions implies an interplay between fibrils and small non-fibrillar material. This may be a result of long fibrils aligning at the air-water interface and smaller aggregates and peptides were subsequently embedded in interstices. Consequently, a dense and stiff fibrillar network was formed. These explanations are consistent with previous studies using pure β-lg fibrils of different lengths [6,22]. Also Jordens and colleagues [10] reported that at pH 2 the purified β-lg fibrils (MWCO = 100 kDa) aligned at the air-water interface into a 2D nematic domain with a strong network formation, creating a highly elastic interface. In this case, 70 % of the interface was occupied by aligned fibrils, while the remaining area was covered by disordered filaments. Because there was significantly less small protein material in AF than in AAS, the higher compressibility of AF could be explained by the absence of small "spacer material" (Fig. 4B). In contrast, no amyloids and aggregates > 300 kDa that could have formed a fibrillar network were present in n-AF, so that here the interfacial film consists only of peptides and small non-amyloid aggregates, which could be comparably more compressed. This is consistent with Rullier and colleagues [16], who suggested for β-lg systems at pH 7 that smaller aggregates and non-aggregated material can behave like anchors at the air-water interface, while larger aggregates can attach to them and mutually stabilize by crosslinking.

Upon further reduction of the trough area (Fig. 4B), a further change in linearly Π-A isotherm slope occurred, which was lower than that of the LE phase. A very well-ordered liquid-condensed phase (LC), as in a two-dimensional liquid crystal, however, would have been indicated by a very sudden and steep increase in Π-A isotherm [43]. Since this was not the case, it is very likely that further compression here led to a mixed regime of LE and LC phases involving semi-crystalline solid and more disordered molecules [44]. These observations are also in agreement with the results of Farrokhi and colleagues [12], who detected semi-crystalline structures by differential scanning calorimetry and X-ray diffraction for fibrillated WPI solutions at pH2, as well as amorphous parts with a glass to rubber transition. This LE/LC transition phase ($A_{T\text{-}LE/LC}$) was achieved significantly earlier by the AAS, n-AF, and AF compared with the two controls, however, the stronger effect of the AAS protein mixture was no longer present. This may indicate that the fibrillar protein structures take longer to align at the air-water interface, but do not further hinder the condensation of the molecules once loosely ordered. This was also the case when lastly, the collapse of the film was considered equivalent for all samples in the range of $A_{T,collapse} = 9.2 \pm 0.2$ cm^2 (Fig. 4B). Because this was very close to the minimum trough area, the reliability of results was reduced.

Although the compression isotherms for the individual protein fractions differed, the expansion isotherms for all samples were comparable (Fig. 4A). The first derivative of the expansion isotherms (*supp. material* Fig. S3) evidenced the same exponential decay for all samples up to an averaged trough area of $A_T = 11.2 \pm 0.8$ cm^2, which may represent the decompression of the molecules until no further outer pressure lays on the molecules. As a consequence, from the different compression and expansion isotherms during one compression-expansion cycle, all samples showed hysteresis. The hysteresis loop area, enclosed between the compression and expansion was similar and

significantly smaller for the UH ($A_H = 12.8 \pm 2.8$ μNm) and STH ($A_H = 17.4 \pm 1.3$ μNm) with below 20 μNm compared with the total amyloid system ($A_H = 34.1 \pm 3.7$ μNm) and its fractions. While isolated fibrils ($A_H = 27.0 \pm 3.9$ μNm) and the AAS resulted in an equivalent hysteresis loop area, the isolated n-AF ($A_H = 23.3 \pm 2.0$ μNm) revealed a significant lower hysteresis than the AAS but not as the AF. Hysteresis loops within a single compression-expansion cycle indicate a slow adjustment of the molecular structure during expansion or a desorption from the film at high surface pressure [7,37]. From repeated cycles, the stability of the film can be concluded [38], but this was not investigated in the present study. Thus, the calculated hysteresis loop area is synonymous with the net negative energy that is lost per compression−expansion cycle [45], which confirmed the assumption that orientation of semi-flexible and larger protein fractions consumes more energy. This was the case in AF, showing the second highest energy loss. In combination with small protein material the energy needed for orientation and assembly of fibrils is equivalent, however, the yield of amyloid fibrils in AAS was only 20 %, clearly indicating the interplay of amyloid and non-amyloid proteins at the air-water interface.

Data thus imply that mixture of semi-flexible fibrils, peptides, non-amyloid aggregates, and monomeric sized proteins in AAS synergistically occupy the air-water interface earlier and denser as pure fibrils or non-structured protein material at the same protein concentration, i.e., lower protein concentration is needed for the same fully occupation of the air-water interface.

3.4. Foaming behavior of amyloid aggregated systems as a function of amyloid and non-amyloid components

The foamability and the foam stability of AAS with varying conversion rates were investigated using a glass foam fractionation column. The foamability describes the general capability of a protein to stabilize foam. With a foam fractionation setup, the foamate volume (V_F) (Fig. 5A) and the mean foamate flow (V_F / *time*) (Fig. 5B) is determined, whereas for both parameters a high value indicates a higher foamability [46]. The highest foamate volume was measured for protein solution with a conversion rate of 10 % ($V_{F,\ 10\ \%} = 19 \pm 1.7$ ml), and it was significantly lower in solutions with higher amyloid fractions ($V_{F,\ 20\ \%} = 14 \pm 0.9$ ml, $V_{F,30\ \%} = 11 \pm 2.9$ ml) (Fig. 5A). The protein concentration in the feed solution was the same for all samples. A similar trend was observed for the mean foamate flow, reaching the highest value at the 10 % conversion rate ($V_{F10\ \%}$ / *time* $= 0.028 \pm 0.001$ ml/s). Only at 30 % vs. 10 % conversion rate was a significant difference, where the mean foamate flow was only half ($V_{F10\ \%}$ / *time* $= 0.014 \pm 0.006$ ml/s) (Fig. 5B). A high V_F, indicates that more water was transported over the entire foaming time. The reason for this could either be that a finer foam with smaller bubbles was present in the column or simply that the foam flow was stable over a longer period of time. In this case, the foaming time alone is not strongly related to the conversion rate, but the foam volume is. AAS with 10 % conversion rate had the highest foam volume, which in combination with the comparable foaming times means that the foam was finer and had a larger specific surface area. Because the protein concentration in the retentate changed only marginally and the feed concentration was the same in all experiments, the amount of transferred protein was approximately constant in all experiments. Thus, it can be concluded that with the same protein concentration a larger air-water interface in the finer foam was stabilized, which is also consistent with the observations in Langmuir film experiments (cf.3.3). On the process side, this observation is the result of a lower surface excess needed for stabilization of the smaller bubbles resulting in a higher foam density [47]. Because of the constant airflow in all experiments, a higher mean foamate flow indicated a higher foam density. The water content was therefore high, which confirms the assumption of thicker films and smaller bubbles [47]. In the case of transient foams, i.e., foams with a lifetime in the range of a few minutes, the foamability and foam stability cannot be considered separately because they are interdependent [48].

The foam stability (Fig. 5C) was expressed as protein concentration in the retentate, the solution remaining in the column after foaming. This in turn indicates that the lower the protein concentration, the less protein is required to stabilize the foam. The lowest protein concentration in the retentate was found at the lowest conversion rate ($c = 0.046 \pm 0.001$ mg/ml), while the highest protein concentration was detected at the highest conversion rate of 30 % ($c = 0.055 \pm 0.002$ mg/ml). This implies longer foam stabilities were achieved in foams containing more non-amyloid components.

The foaming behavior of AAS seems to be dominated by the peptides and peptide aggregates, whose content was higher at the 10 % conversion rate (Fig. 1). Non-amyloid aggregates adsorbed twice as fast at the air-water interface as the fibrils (Fig. 3B) which could be the reason for the better foamability. Further, the less energy was required to assemble in an LE phase in a monolayer (Fig. 4D), which could improve the ability to rapidly stabilize air bubbles. These observations are in line with Wan and colleagues [17] who demonstrated for soy glycine fibril systems that the peptides are responsible for the foaming properties because they moved faster to the interface than the fibrils. Also in a WPI bead system, the smaller constitutes were likely to play the major role on the rheological properties at the air-water interface [49]. Apart from that, the strong electrostatic repulsion and the slower adsorption at the interface of the amyloid aggregates formed at pH 2 [8], might cause the involvement of the fibrils in the foaming process to be very low. This assumption could be further supported by the observations of Oboroceanu and colleagues [18] since they proved that foam stability and foamability were independent of the length of the amyloid fibrils and consequently of the migration rate. Davis and Foegeding [50] investigated in their study that the more polymerized WPI was present, the slower the interfacial tension decreased. Likewise Rullier et al. [15] observed that the amount of aggregates in a mixture of monomeric β lg

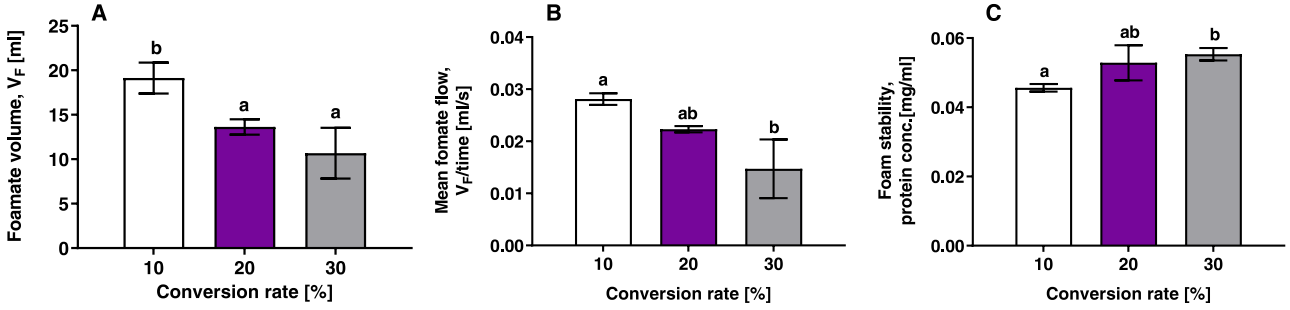

Fig. 5. Foaming of WPI solutions with conversion rates of 10, 20, or 30 %. (A) Foamate volume, foamed in a glass foam fractionation column until the continuous foam flow was interrupted. (B) Mean foamate flow expressed as volume of the foamate per second. (C) Foam stability expressed as the protein concentration of the retentate of WPI solution after foaming. Prior to measurements, all samples were adjusted to a final protein concentration of 0.01 g/100 ml. Different letters indicate statistically significant differences ($n = 3$, $p < 0.05$, Tukey).

and larger aggregates had a strong influence on foam formation and stability. Only 2 % of non-aggregated protein was sufficient to achieve comparable foam formation as in a foam without protein aggregates. At least 10 % monomeric protein was required for foam stability. Only a small amount of non-aggregated protein was sufficient to dominate the foaming properties.

To conclude, the foaming experiments in the present study (Fig. 5) confirmed that improved foam formation and stability occurred if fewer amyloid aggregates were present and the amount of non-amyloid material was increased (Fig. 1). In comparison, the non-amyloid proteins did not show higher hydrophobicity, but stronger adsorption at the air-water interface. (Fig. 3B). That the alignment of a few semi-flexible fibrils in the presence of small protein material in AAS within the monolayer at the air-water interface required more energy than the isolated fibrils (AF) (Fig. 4D) clearly indicates the interplay of amyloid and non-amyloid proteins at the air-water interface. In conclusion, these observations may indicate that the non-amyloid fractions spread more rapidly at the air-water interface and subsequently integrate adherent fibrils into the film formation, further reducing the low flexibility and elasticity of the fibrils by crosslinking. This also strongly confirms the findings of Rullier and colleagues [16] for pure non-amyloid β-lg aggregates, who reported that a network of aggregated and non-aggregated proteins at pH 7 has the advantage of higher viscosity and is therefore less susceptible to drainage. Likewise, Peng and colleagues [51] recently showed in their study using aggregates of β-lactoglobulin-fibril-peptide mixture and gliadin nanoparticles that a denser adsorption layer of proteins at the air-water interface results in a more stable foam with less coalescence, disproportionation, and drainage.

4. Conclusion

We demonstrated that low-concentrate fibrillated WPI systems at pH 2 without separation of the non-amyloid material greatly improved interfacial activity, foamability and foam stability. The initial WPI concentrations governed the ratio of amyloid and non-amyloid fraction, where a ratio with a higher content of non-amyloid material and few fibrils resulted in an optimal interaction at the air-water interface. Faster migration and twice as fast adsorption rate of the smaller non-amyloid material could be the reason for the higher foamability, e.g., in presence of small air bubbles. Apart from the adsorption rate, the less energy required to assemble in an LE phase in a monolayer, i.e., they compress stronger in the monolayer than the fibrils, also improves the ability to rapidly stabilize air bubbles. The diffusion of fibrils was possibly slowed by the high aspect ratio and charge anisotropy but compensated by the high surface hydrophobicity. The higher energy needed of fibril orientation and assembly in a monolayer in the presence of small protein material in AAS than in its absence suggested an interplay between amyloid and non-amyloid proteins at the air-water interface. Non-amyloid fractions can be incorporated into a fibrillar film, which in turn could increase the density and stiffness of the network and thus the interfacial stability of the film. For foams, we suggest that WPI should preferably be used as a fibrillated protein system with low protein concentration, as it synergistically occupies the air-water interface earlier and more densely than pure fibrils or non-structured protein material at the same protein concentration. Omitting the isolation of fibrils will lower the production costs and makes the application of fibrillated systems based on low protein concentration in food more attractive.

Funding

This research is funded by the priority program SPP1934 of the German Research Foundation: DiSPBiotech – dispersity, structural and phase modifications of proteins and biological agglomerates in biotechnological processes, project number 315456892.

CRediT authorship contribution statement

J. Lux: Conceptualization, Methodology, Investigation, Formal analysis, Visualization, Writing – original draft. **H. Kieserling:** Investigation, Writing – review & editing. **J. Koop:** Investigation, Writing – original draft, Writing – review & editing. **S. Drusch:** Writing – review & editing, Supervision, Funding acquisition. **K. Schwarz:** Writing – review & editing, Supervision, Funding acquisition. **J.K. Keppler:** Conceptualization, Writing – original draft, Writing – review & editing, Funding acquisition. **A. Steffen-Heins:** Conceptualization, Methodology, Formal analysis Visualization, Writing – original draft, Writing – review & editing, Supervision, Funding acquisition, Project administration.

Declaration of Competing Interest

The authors declare that they have no known competing financial interests or personal relationships that could have appeared to influence the work reported in this paper.

Data Availability

Data will be made available on request.

Appendix A. Supporting information

Supplementary data associated with this article can be found in the online version at doi:10.1016/j.colsurfa.2022.130849.

References

[1] L. Hoppenreijs, L. Fitzner, T. Ruhmlieb, T.R. Heyn, K. Schild, A.-J. van der Goot, R. M. Boom, A. Steffen-Heins, K. Schwarz, J.K. Keppler, Engineering amyloid and amyloid-like morphologies of β-lactoglobulin, Food Hydrocoll. 124 (2022), 107301, https://doi.org/10.1016/j.foodhyd.2021.107301.

[2] Jianxiong Yue, Xiaolin Yao, Qingxia Gou, Dan Li, Ning Liu, Dan Yang, et al., Recent advances of interfacial and rheological property based techno-functionality of food protein amyloid fibrils (S), Food Hydrocoll. 132 (2022), 107827, https://doi.org/10.1016/j.foodhyd.2022.107827.

[3] Mehdi Mohammadian, Ashkan Madadlou, Technological functionality and biological properties of food protein nanofibrils formed by heating at acidic condition, Trends Food Sci. Technol. 75 (2018) S.115–S.128, https://doi.org/10.1016/j.tifs.2018.03.013.

[4] C. Akkermans, P. Venema, A.J. van der Goot, H. Gruppen, E.J. Bakx, R.M. Boom, E. van der Linden, Peptides are building blocks of heat-induced fibrillar protein aggregates of beta-lactoglobulin formed at pH 2, Biomacromolecules 9 (2008) 1474–1479, https://doi.org/10.1021/bm7014224.

[5] T.R. Heyn, V.M. Garamus, H.R. Neumann, M.J. Uttinger, T. Guckeisen, M. Heuer, C. Selhuber-Unkel, W. Peukert, J.K. Keppler, Influence of the polydispersity of pH 2 and pH 3.5 beta-lactoglobulin amyloid fibril solutions on analytical methods, Eur. Polym. J. (2019), https://doi.org/10.1016/j.eurpolymj.2019.08.038.

[6] J.-M. Jung, D.Z. Gunes, R. Mezzenga, Interfacial activity and interfacial shear rheology of native β-lactoglobulin monomers and their heat-induced fibers, Langmuir 26 (2010) 15366–15375, https://doi.org/10.1021/la102721m.

[7] Z. Wang, G. Narsimhan, Interfacial dilatational elasticity and viscosity of beta-lactoglobulin at air-water interface using pulsating bubble tensiometry, Langmuir 21 (2005) 4482–4489, https://doi.org/10.1021/la047374g.

[8] D. Peng, J. Yang, J. Li, C. Tang, B. Li, Foams stabilized by β-lactoglobulin amyloid fibrils: effect of pH, J. Agric. Food Chem. 65 (2017) 10658–10665, https://doi.org/10.1021/acs.jafc.7b03669.

[9] J. Hu, J. Yang, Y. Xu, K. Zhang, K. Nishinari, G.O. Phillips, Y. Fang, Comparative study on foaming and emulsifying properties of different beta-lactoglobulin aggregates, Food Funct. 10 (2019) 5922–5930, https://doi.org/10.1039/C9FO00940J.

[10] S. Jordens, P.A. Rühs, C. Sieber, L. Isa, P. Fischer, R. Mezzenga, Bridging the gap between the nanostructural organization and macroscopic interfacial rheology of amyloid fibrils at liquid interfaces, Langmuir 30 (2014) 10090–10097, https://doi.org/10.1021/la5020658.

[11] Oboroceanu D., Wang L., Magner E., Auty M.A. Fibrillization of whey proteins improves foaming capacity and foam stability at low protein concentrations. Journal of Food Engineering, 121, pp. 102–111. ⟨https://doi.org/10.1016/j.jfoodeng.2013.08.023⟩.

[12] Flora Farrokhi, Mohammad Reza Ehsani, Fojan Badii, Maryam Hashemi, Structural and thermal properties of nanofibrillated whey protein isolate in the glassy state, LWT 95 (2018) S.274–S.281, https://doi.org/10.1016/j.lwt.2018.05.001.

[13] Yunchun Diao, Yanpeng Zhang, Weinong Zhang, Wei Xu, Zhixiong Hu, Yang Yi, Yuehui Wang, Acid-thermal-induced formation of rice bran protein nano-particles:

foaming properties and physicochemical characteristics, Int. J. Food Sci. Technol. 57 (6) (2022) S.3624–S.3633, https://doi.org/10.1111/ijfs.15686.
[14] Yanpeng Zhang, Yunchun Diao, Weinong Zhang, Wei Xu, Zhixiong Hu, Yang Yi, Influence of molecular structure and interface behavior on foam properties of rice bran protein nano-particles, LWT 163 (2022), S.113537, https://doi.org/10.1016/j.lwt.2022.113537.
[15] B. Rullier, B. Novales, M.A. Axelos, Effect of protein aggregates on foaming properties of β-lactoglobulin, Colloids Surf. A: Physicochem. Eng. Asp. 330 (2–3) (2008) 96–102, https://doi.org/10.1016/j.colsurfa.2008.07.040.
[16] B. Rullier, M.A.V. Axelos, D. Langevin, B. Novales, Effect of protein aggregates on foaming properties of β-lactoglobulin, Colloids Surf. A: Physicochem. Eng. Asp. 330 (2008) 96–102, https://doi.org/10.1016/j.colsurfa.2008.07.040.
[17] Z. Wan, X. Yang, L.M.C. Sagis, Contribution of Long Fibrils and Peptides to Surface and Foaming Behavior of Soy Protein Fibril System, Langmuir 32 (2016) 8092–8101, https://doi.org/10.1021/acs.langmuir.6b01511.
[18] D. Oboroceanu, L. Wang, E. Magner, M.A. Auty, Fibrillization of whey proteins improves foaming capacity and foam stability at low protein concentrations, J. Food Eng. 121 (2014) 102–111, https://doi.org/10.1016/j.jfoodeng.2013.08.023.
[19] F. Farrokhi, F. Badii, M.R. Ehsani, M. Hashemi, Functional and thermal properties of nanofibrillated whey protein isolate as functions of denaturation temperature and solution pH, Colloids Surf. A: Physicochem. Eng. Asp. 583 (2019), 124002, https://doi.org/10.1016/j.colsurfa.2019.124002.
[20] M. Mohammadian, A. Madadlou, Characterization of fibrillated antioxidant whey protein hydrolysate and comparison with fibrillated protein solution, Food Hydrocoll. 52 (2016) 221–230, https://doi.org/10.1016/j.foodhyd.2015.06.022.
[21] X. Ye, M.S. Hedenqvist, M. Langton, C. Lendel, On the role of peptide hydrolysis for fibrillation kinetics and amyloid fibril morphology, RSC Adv. 8 (2018) 6915–6924, https://doi.org/10.1039/C7RA10981D.
[22] Y. Serfert, C. Lamprecht, C.-P. Tan, J.K. Keppler, E. Appel, F.J. Rossier-Miranda, K. Schroen, R.M. Boom, S. Gorb, C. Selhuber-Unkel, S. Drusch, K. Schwarz, Characterisation and use of β-lactoglobulin fibrils for microencapsulation of lipophilic ingredients and oxidative stability thereof, J. Food Eng. 143 (2014) 53–61, https://doi.org/10.1016/j.jfoodeng.2014.06.026.
[23] F. Tamm, G. Sauer, M. Scampicchio, S. Drusch, Pendant drop tensiometry for the evaluation of the foaming properties of milk-derived proteins, Food Hydrocoll. 27 (2012) 371–377, https://doi.org/10.1016/j.foodhyd.2011.10.013.
[24] H. Schestkowa, T. Wollborn, A. Westphal, A. Maria Wagemans, U. Fritsching, S. Drusch, Conformational state and charge determine the interfacial stabilization process of beta-lactoglobulin at preoccupied interfaces, J. Colloid Interface Sci. 536 (2019) 300–309, https://doi.org/10.1016/j.jcis.2018.10.043.
[25] I. Barackov, A. Mause, S. Kapoor, R. Winter, G. Schembecker, B. Burghoff, Investigation of structural changes of β-casein and lysozyme at the gas-liquid interface during foam fractionation, J. Biotechnol. 161 (2012) 138–146, https://doi.org/10.1016/j.jbiotec.2012.01.030.
[26] P.J. Halling, Protein-stabilized foams and emulsions, Crit. Rev. Food Sci. Nutr. 15 (1981) 155–203, https://doi.org/10.1080/10408398109527315.
[27] S.G. Bolder, A.J. Vasbinder, L.M. Sagis, E. van der Linden, Fibril assemblies in aqueous whey protein mixtures, J. Agric. Food Chem. 54 (2006) 4229–4234, https://doi.org/10.1021/jf060606s.
[28] C. Veerman, H. Ruis, L. Sagis, E. van der Linden, Effect of electrostatic interactions on the percolation concentration of fibrillar β-lactoglobulin gels, Biomacromolecules (2002) 869–873, https://doi.org/10.1021/bm025533.
[29] Keppler J.K., Heyn T.R., Meissner P.M., Schrader K., Schwarz K. Protein oxidation during temperature-induced amyloid aggregation of beta-lactoglobulin. Food Chemistry, 289, pp. 223–231. ⟨https://doi.org/10.1016/j.foodchem.2019.02.114⟩.
[30] S.G. Bolder, H. Hendrickx, L.M.C. Sagis, E. van der Linden, Fibril assemblies in aqueous whey protein mixtures, J. Agric. Food Chem. 54 (2006) 4229–4234, https://doi.org/10.1021/jf060606s.
[31] J. Lux, M. Azarkh, L. Fitzner, J.K. Keppler, K. Schwarz, M. Drescher, A. Steffen-Heins, Amyloid aggregation of spin-labeled β-lactoglobulin. Part II: Identification of spin-labeled protein and peptide sequences after amyloid aggregation, Food Hydrocoll. 112 (2021), 106174, https://doi.org/10.1016/j.foodhyd.2020.106174.
[32] J. Lux, T.R. Heyn, I. Kampen, K. Schwarz, J.K. Keppler, A. Steffen-Heins, Amyloid aggregation of spin-labeled β-lactoglobulin. Part I: Influence of spin labeling on amyloid aggregation, Food Hydrocoll. 112 (2021), 106178, https://doi.org/10.1016/j.foodhyd.2020.106178.
[33] P.J. Atkinson, E. Dickinson, D.S. Horne, R.M. Richardson, Neutron reflectivity of adsorbed β-casein and β-lactoglobulin at the air/water interface, J. Chem. Soc. Faraday Trans. 91 (1995) 2847–2854, https://doi.org/10.1039/FT9959102847.
[34] G. Unterhaslberger, C. Schmitt, C. Sanchez, C. Appolonia-Nouzille, A. Raemy, Heat denaturation and aggregation of β-lactoglobulin enriched WPI in the presence of arginine HCl, NaCl and guanidinium HCl at pH 4.0 and 7.0, Food Hydrocoll. 20 (2006) 1006–1019, https://doi.org/10.1016/j.foodhyd.2005.10.017.
[35] A.F.H. Ward, L. Tordai, Time-dependence of boundary tensions of solutions I. The role of diffusion in time-effects, J. Chem. Phys. 14 (1946) 453–461, https://doi.org/10.1063/1.1724167.
[36] J.K. Keppler, A. Steffen-Heins, C.C. Berton-Carabin, M.-H. Ropers, K. Schwarz, Functionality of whey proteins covalently modified by allyl isothiocyanate. Part 2: Influence of the protein modification on the surface activity in an O/W system, Food Hydrocoll. 81 (2018) 286–299, https://doi.org/10.1016/j.foodhyd.2018.03.003.
[37] W.R. Glomm, S. Volden, Ø. Halskau, M.-H.G. Ese, Same system-different results: The importance of protein-introduction protocols in Langmuir-monolayer studies of lipid-protein interactions, Anal. Chem. 81 (2009) 3042–3050, https://doi.org/10.1021/ac8027257.
[38] N.F. Crawford, R.M. Leblanc, Serum albumin in 2D: A Langmuir monolayer approach, Adv. Colloid Interface Sci. 207 (2014) 131–138, https://doi.org/10.1016/j.cis.2013.10.021.
[39] W.D. Harkins, T.F. Young, E. Boyd, The thermodynamics of films: energy and entropy of extension and spreading of insoluble monolayers, J. Chem. Phys. 8 (1940) 954–965, https://doi.org/10.1063/1.1750610.
[40] D. Vollhardt, V.B. Fainerman, Progress in characterization of Langmuir monolayers by consideration of compressibility, Adv. Colloid Interface Sci. 127 (2006) 83–97, https://doi.org/10.1016/j.cis.2006.11.006.
[41] M. Ikeguchi, S. Kato, A. Shimizu, S. Sugai, Molten globule state of equine β-Lactoglobulin, Proteins 27 (1997) 567–575, https://doi.org/10.1002/(SICI)1097-0134(199704)27:4<567:AID-PROT9>3.0.CO;2-7.
[42] J.K. Keppler, D. Martin, V.M. Garamus, C. Berton-Carabin, E. Nipoti, T. Coenye, K. Schwarz, Functionality of whey proteins covalently modified by allyl isothiocyanate. Part 1 physicochemical and antibacterial properties of native and modified whey proteins at pH 2 to 7, Food Hydrocoll. 65 (2017) 130–143, https://doi.org/10.1016/j.foodhyd.2016.11.016.
[43] S.L. Duncan, R.G. Larson, Comparing experimental and simulated pressure-area isotherms for DPPC, Biophys. J. 94 (2008) 2965–2986, https://doi.org/10.1529/biophysj.107.114215.
[44] J. Nepal B, K. Stine, Monolayers of carbohydrate-containing lipids at the water- air interface, in: R.A. Mehanna (Ed.), Cell Culture, IntechOpen, London, 2019, https://doi.org/10.5772/intechopen.76440.
[45] L. Xu, Y.Y. Zuo, Reversible phase transitions in the phospholipid monolayer, Langmuir 34 (2018) 8694–8700, https://doi.org/10.1021/acs.langmuir.8b01544.
[46] J. Koop, J. Merz, R. Wilmshöfer, R. Winter, G. Schembecker, Influence of thermally induced structure changes in diluted β-lactoglobulin solutions on their surface activity and behavior in foam fractionation, J. Biotechnol. 319 (2020) 61–68, https://doi.org/10.1016/j.jbiotec.2020.05.011.
[47] A. Hofmann, G. Schembecker, J. Merz, Role of bubble size for the performance of continuous foam fractionation in stripping mode, Colloids Surf. A: Physicochem. Eng. Asp. 473 (2015) 85–94, https://doi.org/10.1016/j.colsurfa.2014.12.042.
[48] J. Wang, A.V. Nguyen, S. Farrokhpay, A critical review of the growth, drainage and collapse of foams, Adv. Colloid Interface Sci. 228 (2016) 55–70, https://doi.org/10.1016/j.cis.2015.11.009.
[49] J. Yang, I. Thielen, C.C. Berton-Carabin, E. van der Linden, L.M. Sagis, Nonlinear interfacial rheology and atomic force microscopy of air-water interfaces stabilized by whey protein beads and their constituents, Food Hydrocoll. 101 (2020), 105466, https://doi.org/10.1016/j.foodhyd.2019.105466.
[50] J.P. Davis, E.A. Foegeding, Foaming and interfacial properties of polymerized whey protein isolate, J. Food Sci. 69 (2004) C404–C410, https://doi.org/10.1111/j.1365-2621.2004.tb10706.x.
[51] Dengfeng Peng, Weiping Jin, Leonard M.C. Sagis, Bin Li, Adsorption of microgel aggregates formed by assembly of gliadin nanoparticles and a β-lactoglobulin fibril-peptide mixture at the air/water interface: Surface morphology and foaming behavior, Food Hydrocoll. 122 (2022), S.107039, https://doi.org/10.1016/j.foodhyd.2021.107039.